Bistability of a two-dimensional Klein-Gordon system as a reliable means to transmit monochromatic waves: A numerical approach

Jorge Eduardo Macías-Díaz*

Departamento de Matemáticas y Física, Universidad Autónoma de Aguascalientes, Avenida Universidad 940, Colonia Ciudad Universitaria, Aguascalientes, Ags. 20100, México

(Received 6 August 2008; revised manuscript received 29 September 2008; published 12 November 2008)

Departing from a reliable computational method to approximate solutions of dissipative, nonlinear wave equations, we study the bistability of a (2+1)-dimensional sine-Gordon system, spatially defined on a bounded square of the first quadrant of the Cartesian plane, and subject to Dirichlet boundary data in the form of harmonic driving on the coordinate axes, oscillating at a frequency in the forbidden band gap of the medium. It is shown numerically that, as its spatially discrete counterpart, the continuous (2+1)-dimensional sine-Gordon equation presents the process of nonlinear supratransmission, and that this phenomenon is independent of the discretization procedure. Moreover, our simulations show that a bistable region, where a conducting state and an insulating state may coexist, is present in this system, even in the presence of external damping. As an application, it is shown that the bistable regime may be properly employed in order to transmit certain monochromatic waves through these media.

DOI: 10.1103/PhysRevE.78.056603 PACS number(s): 05.45.Yv, 02.60.Lj, 45.10.−b, 63.20.Pw

I. INTRODUCTION

The (1+1)-dimensional sine-Gordon equation is a partial differential equation that has been thoroughly studied in the mathematical (both analytically and numerically) and physical literatures. However, this equation is far from being completely understood, and time has come to show that new and fascinating properties of the sine-Gordon equation are frequently discovered.

One of the properties of the sine-Gordon equation that was recently unveiled is the so-called phenomenon of nonlinear supratransmission [1], which consists in a sudden increase in the amplitude of wave signals in a bounded or semiunbounded medium, subject to harmonic driving in the boundary. It has been shown analytically and numerically [2,3] that both Neumann and Dirichlet boundary data in the form of sinusoidal perturbations are able to induce the presence of supratransmission. Moreover, nowadays we know that other systems, such as Fermi-Pasta-Ulam discrete chains [4], also present nonlinear supratransmission, and it has been suggested that every nonlinear system may be able to present it as long as it possesses a natural, forbidden band gap.

In addition to nonlinear supratransmission, the (1+1)-dimensional sine-Gordon equation has been shown to present another quite interesting property: nonlinear bistability. This property is characterized by the coexistence of two stationary states, called conducting and insulating regimes. More precisely, if starting from a value of zero we slowly increase the driving amplitude of a (bounded or semiunbounded) medium subject to harmonic driving in one end at a frequency Ω in the forbidden band gap, then the existence of a critical value A_s at which the medium starts to absorb energy from the boundary is observed. The value A_s is called the supratransmission threshold, and it marks the transition from an insulating to a conducting regime. Moreover, if the driving amplitude is then decreased after reaching the critical amplitude A_s, the medium still continues to absorb energy from the boundary until the amplitude reaches a second critical value $A_l < A_s$ called the lower-transmission or infratransmission threshold, below which the boundary finally stops irradiating energy into the system. This is nonlinear bistability.

Nonlinear bistability has been discovered in many nonlinear systems. For instance, it has been found in the Duffing equation with nonlinear damping term, an equation important in the modeling of nanomechanical resonators [5]. Also, it has been used in the design of light detectors sensitive to very weak excitations, where the underlying theory is based on a nonlinear Schrödinger equation [6], and in the study of nonlinear effects in semiconductor ring resonators [7]; however, nonlinear bistability historically was discovered in Bragg media driven in the nonlinear Kerr regime [8].

All of the works cited above share a characteristic in common: They study nonlinear media in one (discrete or continuous) space dimension. It is an interesting problem to investigate the presence of bistability in media with two or three space dimensions, which is a topic of research that has not been fully attacked yet. In this paper, we study numerically the nonlinear bistability of a (2+1)-dimensional, continuous sine-Gordon equation with spatial domain confined in a bounded square of the first quadrant of $\mathbb{R}^2$, when two adjacent boundaries lie on the coordinate axes.

It is important to mention that the present work is motivated by the study of the spatially discrete, (1+1)-dimensional systems that arise in the investigation of arrays of parallel Josephson junctions connected through superconducting wires and perturbed harmonically at one end [3], and the investigation of semi-infinite linear arrays of pendula attached by springs and harmonically driven at the end [1]. The study on linear arrays of harmonic oscillators is the source of motivation of the present work, and it is described by the system of ordinary differential equations

*jemacias@correo.uaa.mx

$$\ddot{u}_n - c^2\nabla_x^2 u_n + \gamma\dot{u}_n + \sin u_n = 0 \quad (n \in \mathbb{Z}^+), \tag{1}$$

subject to the boundary condition $u_0=\varphi$, where $\varphi(t)=A\sin(\Omega t)$. Here, the time-dependent real function u_n physically represents the gauge invariant phase difference [9], and $\nabla_x^2 u_n$ denotes the finite second difference $u_{n+1}-2u_n+u_{n-1}$. Both the coupling coefficient c and the damping coefficient are assumed to be nonnegative numbers and $\Omega<1$.

In Sec. II of this work, we present the partial differential equation that represents our point of departure—the continuous, (2+1)-dimensional sine-Gordon equation with damping—and take this opportunity to introduce the energy equation of the system under study. In Sec. III, we quote the finite-difference schemes employed to approximate solutions to the problem in this work, and the total energy of the system. Simulations are presented in the following section. There, we establish numerically the presence of nonlinear supratransmission in the medium of interest, stating that its presence is independent of the discretization process. In one of the outcomes of our investigation, we find computational evidence of the existence of a region of bistability, and hysteresis diagrams are constructed as one of the interesting results of our work.

Section V presents an application of nonlinear bistability to the efficient propagation of monochromatic waves in (2+1)-dimensional sine-Gordon media confined in a bounded domain of $\mathbb{R}^2$. In Sec. VI, we give a brief discussion of our results, in view of the analytical and numerical evidence of bistability in (1+1)-dimensional, continuous media governed by sine-Gordon equations [2,3]. Finally, we close this work with a section of concluding remarks and proposed directions of research.

II. MATHEMATICAL MODEL

We let u be a function of (x,y,t), where x and y take values on the closed interval $[0,L]$, for some $L>0$, and t is restricted to be a nonnegative variable. Moreover, we let γ be a fixed nonnegative real number that will physically represent a coefficient of damping. The problem under study in this work is the following initial-boundary value problem

$$\frac{\partial^2 u}{\partial t^2} - \nabla^2 u + \gamma\frac{\partial u}{\partial t} + G'(u) = 0,$$
$$\text{s.t.}\begin{cases} \dfrac{\partial u(\mathbf{x},0)}{\partial t} = u(\mathbf{x},0) = 0, & \mathbf{x} \in D, \\ u(\mathbf{x},t) = A\sin(\Omega t), & \mathbf{x} \in \partial D_1, \\ \hat{\mathbf{n}}\cdot\nabla u(\mathbf{x},t) = 0, & \mathbf{x} \in \partial D_2, \end{cases} \tag{2}$$

where ∇^2 represents the two-dimensional Laplacian operator, ∇ is the gradient vector, D denotes the closed square $[0,L]\times[0,L]\subset\mathbb{R}^2$, $\hat{\mathbf{n}}$ is the unitary vector normal to the boundary ∂D of D, ∂D_1 is the portion of the boundary of D that coincides with the x or the y axis, $\partial D_2=\partial D\setminus\partial D_1$, and G is a continuously differentiable real function over all $\mathbb{R}$.

The partial differential equation in Eq. (2) is clearly a generalization of the (2+1)-dimensional dissipative sine-Gordon equation, which is a regime that has been widely studied in the specialized literature: analytically [10–13], numerically [14–16], and physically [17–21]. The conservative regime has a forbidden band gap $\Omega<1$, and it has been established that the spatially discrete form of Eq. (2) has the property that such a medium subject to a harmonic driving in the boundary with a frequency Ω presents the phenomenon of transmission of energy in the form of localized nonlinear modes [14].

It is indispensable to point out that the total energy of a conservative system governed by the partial differential equation in Eq. (2) is given by the formula

$$E = \int\int_D H d\mathbf{x}. \tag{3}$$

Here, the local energy density H is provided by the expression

$$H = \frac{1}{2}\left(\frac{\partial u}{\partial t}\right)^2 + \frac{1}{2}\|\nabla u\|^2 + G(u), \tag{4}$$

where $\|\cdot\cdot\|$ is the Euclidean norm in $\mathbb{R}^2$. As a consequence, the derivative of the total energy with respect to time is calculated through

$$E'(t) = \int_{\partial D}\frac{\partial u}{\partial t}\nabla u\cdot\hat{\mathrm{n}}ds - \gamma\int\int_D\left(\frac{\partial u}{\partial t}\right)^2 d\mathbf{x}, \tag{5}$$

where obviously the first integral in the right-hand side of Eq. (5) is a contour integral.

III. COMPUTATIONAL TECHNIQUE

In this section, we briefly describe the numerical method used to approximate solutions to Eq. (2) over a time interval $[0,T]$, for T a positive number. Let $0=x_0<x_1<\cdots<x_M=L$ and $0=y_0<y_1<\cdots<y_N=L$ be two regular partitions of the interval $[0,L]$, of norms $\Delta x=L/M$ and $\Delta y=L/N$, respectively, and let $0=t_1<t_1<\cdots<t_P=T$ be a regular partition of $[0,T]$ of norm $\Delta t=T/P$. Let $u_{m,n}^k$ be the approximation to the exact value of u at the point $(m\Delta x,n\Delta y)$ and time t_k, and let

$$\phi_k = A\sin(\Omega t_k). \tag{6}$$

To approximate solutions to Eq. (2), we employ the finite-difference scheme

$$\frac{\delta_t^2 u_{m,n}^k}{(\Delta t)^2} - \frac{1}{2}\left[\frac{\bar{\delta}_t\delta_x^2 u_{m,n}^k}{(\Delta x)^2} + \frac{\bar{\delta}_t\delta_y^2 u_{m,n}^k}{(\Delta y)^2}\right] + \frac{\gamma}{2\Delta t}\delta_t u_{m,n}^k + \frac{G(u_{m,n}^{k+1}) - G(u_{m,n}^{k-1})}{u_{m,n}^{k+1} - u_{m,n}^{k-1}} = 0,$$
$$\text{s.t.}\begin{cases} u_{m,n}^0 = u_{m,n}^1 = 0, \\ u_{m,0}^k = u_{0,n}^k = \phi_k, \\ u_{M,n}^k - u_{M-1,N}^k = 0, \\ u_{m,N}^k - u_{m,N-1}^k = 0, \end{cases} \tag{7}$$

where G represents the potential of the sine-Gordon system (2), namely, $G(u)=1-\cos u$. Here, the following notation was adopted for the sake of simplicity:

$$\delta_t u_{m,n}^k = u_{m,n}^{k+1} - u_{m,n}^{k-1},$$

$$\bar{\delta}_t u_{m,n}^k = u_{m,n}^{k+1} + u_{m,n}^{k-1},$$

$$\delta_t^2 u_{m,n}^k = u_{m,n}^{k+1} - 2u_{m,n}^k + u_{m,n}^{k-1},$$

$$\delta_x u_{m,n}^k = u_{m+1,n}^k - u_{m,n}^k,$$

$$\delta_x^2 u_{m,n}^k = u_{m+1,n}^k - 2u_{m,n}^k + u_{m-1,n}^k,$$

$$\delta_y u_{m,n}^k = u_{m,n+1}^k - u_{m,n}^k,$$

$$\delta_y^2 u_{m,n}^k = u_{m,n+1}^k - 2u_{m,n}^k + u_{m,n-1}^k. \tag{8}$$

The operators just defined are assumed to be additive and homogeneous, and their compositions are defined in the traditional way.

The method presented here is a variation of the computational technique employed to approximate solutions of a spatially discrete sine-Gordon system [14]. It is important to mention that our technique is consistent with the problem, conditionally stable, and has a consistent energy scheme associated with it, which has the property of consistently approximating the rate of change of energy with respect to time, namely,

$$E_k = \sum_{m=1}^{M-1}\sum_{n=1}^{N-1} H_{m,n}^k \Delta x \Delta y + \frac{1}{4}\sum_{m=1}^{M-1}\left[\frac{(\delta_y u_{m,0}^{k+1})^2 + (\delta_y u_{m,0}^k)^2}{2(\Delta y)^2}\right]\Delta x \Delta y + \frac{1}{4}\sum_{n=1}^{N-1}\left[\frac{(\delta_x u_{0,n}^{k+1})^2 + (\delta_x u_{0,n}^k)^2}{2(\Delta x)^2}\right]\Delta x \Delta y, \tag{9}$$

where the discrete Hamiltonian $H_{m,n}$ is given by the formula

$$\begin{aligned} H_{m,n}^k = {} & \frac{1}{2}\left(\frac{u_{m,n}^{k+1} - u_{m,n}^k}{\Delta t}\right)^2 + \frac{1}{8(\Delta x)^2}[(\delta_x u_{m,n}^{k+1})^2 + (\delta_x u_{m-1,n}^{k+1})^2 \\ & + (\delta_x u_{m,n}^k)^2 + (\delta_x u_{m-1,n}^k)^2] + \frac{1}{8(\Delta y)^2}[(\delta_y u_{m,n}^{k+1})^2 \\ & + (\delta_y u_{m,n-1}^{k+1})^2 + (\delta_y u_{m,n}^k)^2 + (\delta_y u_{m,n-1}^k)^2] \\ & + \frac{G(u_{m,n}^{k+1}) + G(u_{m,n}^k)}{2}. \end{aligned} \tag{10}$$

It is readily checked that finite-difference schemes (7), (10), and (9) are consistent approximations of the continuous formulas (2), (4), and (3), respectively. Moreover, scheme (10) is always nonnegative, a characteristic which is in agreement with the fact that Eq. (4) is positive definite. Also, an algebraic manipulation of the discrete schemes shows that the discrete rate of change of energy is given by the identity

$$\begin{aligned} \frac{E_k - E_{k-1}}{\Delta t} = {} & -\sum_{m=1}^{M-1}\left(\frac{\bar{\delta}\delta_y u_{m,0}^k}{2\Delta y}\right)\frac{\delta_t u_{m,0}^k}{2\Delta t}\Delta x \\ & - \sum_{n=1}^{N-1}\left(\frac{\bar{\delta}\delta_x u_{0,n}^k}{2\Delta x}\right)\frac{\delta_t u_{0,n}^k}{2\Delta t}\Delta y \\ & - \gamma\sum_{m=1}^{M-1}\sum_{n=1}^{N-1}\left(\frac{\delta_t u_{m,n}^k}{2\Delta t}\right)^2 \Delta x \Delta y, \end{aligned} \tag{11}$$

which is a consistent estimation of the derivative of the energy of medium (2) presented as Eq. (5). As a consequence, the discrete energy is conserved for a conservative, undamped medium (2) in which the boundary condition on ∂D_1 is constant.

IV. SIMULATIONS

A. Nonlinear supratransmission

It is known that the process of nonlinear supratransmission is present in discrete, (2+1)-dimensional systems consisting of coupled sine-Gordon equations, with two adjacent boundaries harmonically perturbed by a frequency in the forbidden band gap [14]. We now proceed to verify computationally that this phenomenon is also present in continuous, (2+1)-dimensional sine-Gordon problems such as Eq. (2). So let us fix a spatial domain $[0,L]\times[0,L]$ with $L=5$, consider problem (2) with no damping and driving frequency equal to 0.9, and choose two different driving amplitudes $A=0.99$ and 1.00. From a computational perspective, we set $\Delta t=0.025$ and $\Delta x=\Delta y=0.25$, and fix a time interval [0, 500]. Moreover, in order to avoid the creation of shock waves in the medium due to the abrupt change from a stationary regime to one in which the boundary moves vertically at an initial velocity equal to $A\Omega$, we opt to slowly and linearly increase the value of the driving amplitude from 0 to its actual value A, on the time interval [0, 10].

Under these circumstances, Fig. 1 presents the graph of the solution u at time 451.5, versus the spatial variables x and y. The left graph represents the solution corresponding to a driving amplitude equal to 0.99, while the right graph presents the solution corresponding to an amplitude equal to 1.00. The results show the presence of a drastic change in the qualitative nature of the solutions, at least when $\Omega=0.9$. We have run simulations for other values of A around the critical value 1.00, and have concluded that this value constitutes indeed a threshold value, above which the creation of localized nonlinear solutions is triggered.

Before moving forward in our investigation, it is important to mention that time $t=451.5$ was chosen by virtue of the fact that it is around this instant when the sine-Gordon system driven with an amplitude of 1.00 reaches its highest maximum in the experiment described above. A numerical determination of the smallest time at which supratransmission shows up in a system described by Eq. (2) will be carried out at the end of the present section.

As a means to verify our observations, we have focused our attention on the development of solutions on the straight line $y=x$. Figure 2 depicts the time evolution of solutions

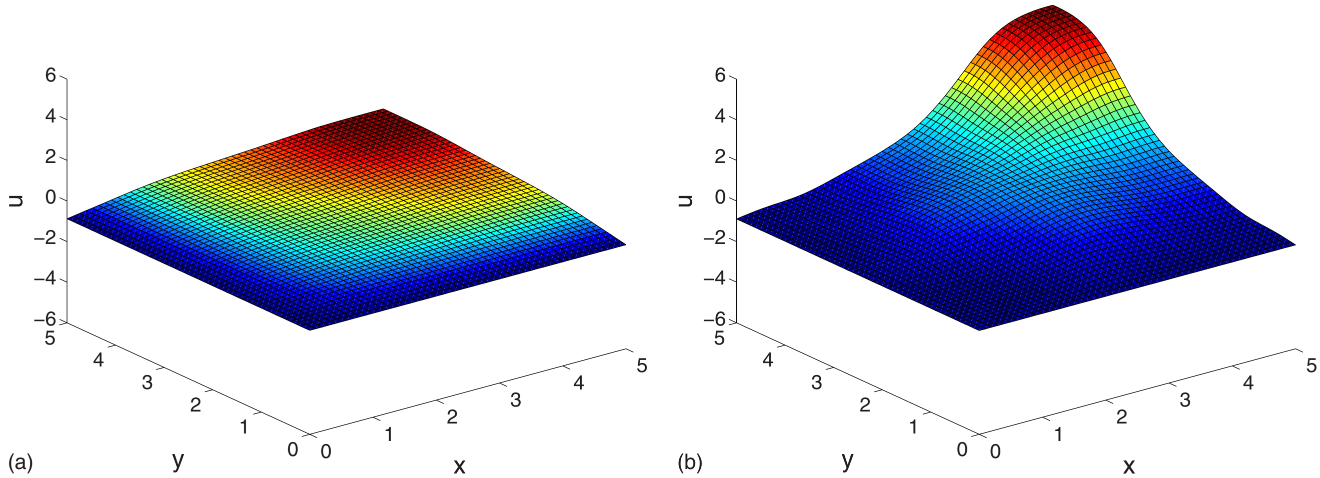

FIG. 1. (Color online) Graph of the solution u versus x and y, corresponding to undamped, initial-boundary-value problem (2), at time 451.5. A driving frequency Ω equal to 0.9 was fixed, and two different driving amplitudes have been chosen: $A=0.99$ (left) and 1.00 (right). The graphs show the presence of nonlinear supratransmission in continuous, (2+1)-dimensional sine-Gordon equations.

(presented in the top row) and local energy densities (bottom row) of an undamped medium governed by Eq. (2) restricted to the spatial domain $y=x$ and the time interval [450, 500], for the two different amplitude values studied in the previous paragraph, and driving frequency equal to 0.9. For a diving amplitude equal to 0.99, our computations show that the solution to the problem is clearly bounded by 3 and that the local energy density is nonnegative and bounded by 1. How-

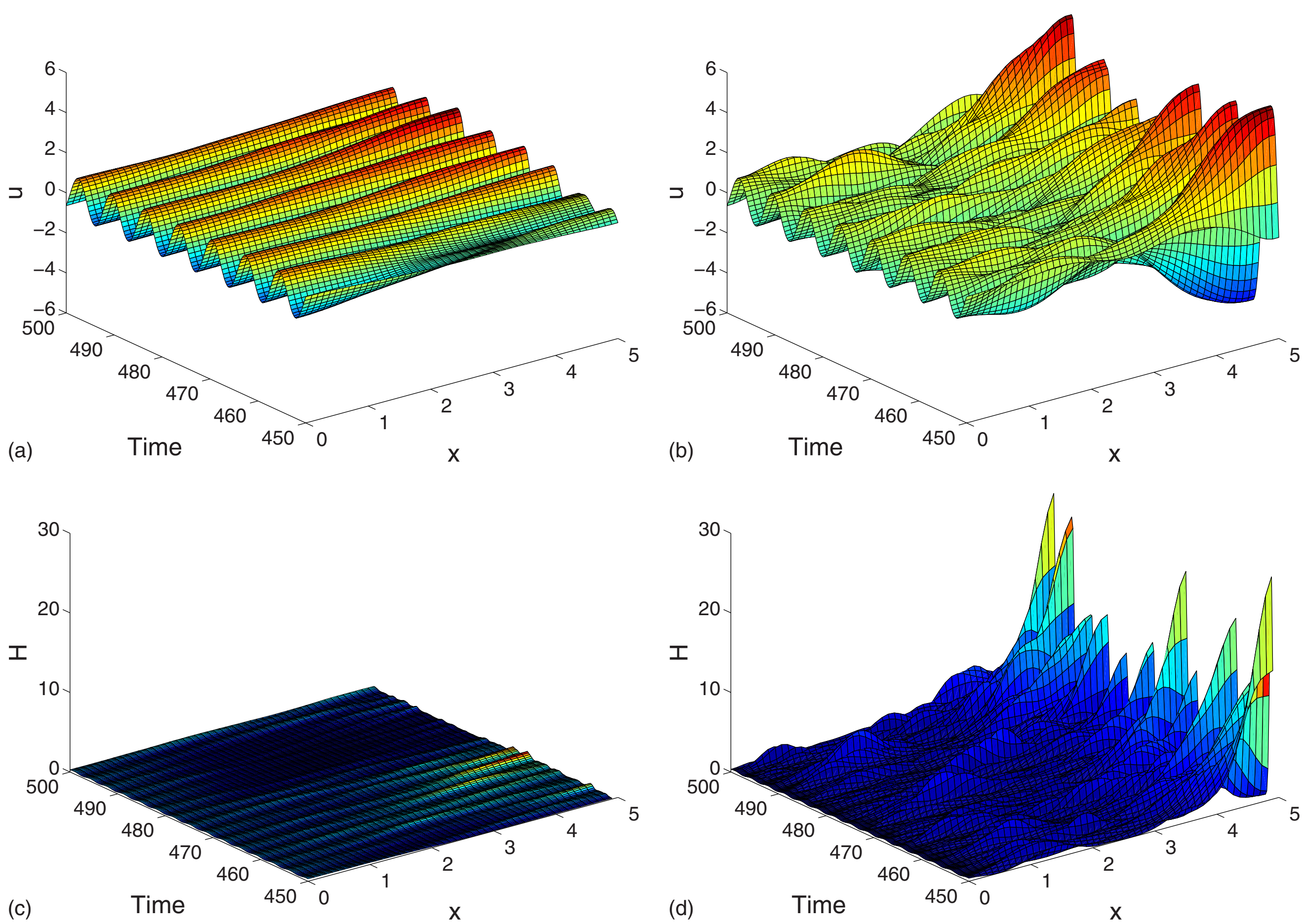

FIG. 2. (Color online) Time-dependent graphs of the solution u (top row) and the local energy density (bottom row) of Eq. (2) along the line $y=x$, for a system with no damping, defined in the spatial domain $[0,5]\times[0,5]$. A driving frequency $\Omega=0.9$ was fixed, and two different driving amplitudes were chosen: one right before supraransmission occurs ($A=0.99$, left column), and the other after it has already taken place ($A=1.00$, right column).

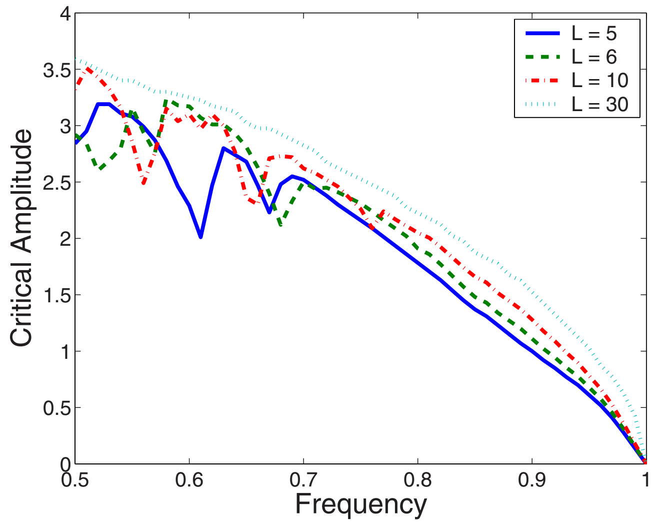

FIG. 3. (Color online) Diagrams of occurrence of critical amplitude at which supratransmission starts versus driving frequency, for an undamped, two-dimensional sine-Gordon problem (2) defined spatially in the set $[0,L]\times[0,L]$, for several values of L. The system is harmonically perturbed on the coordinate axes.

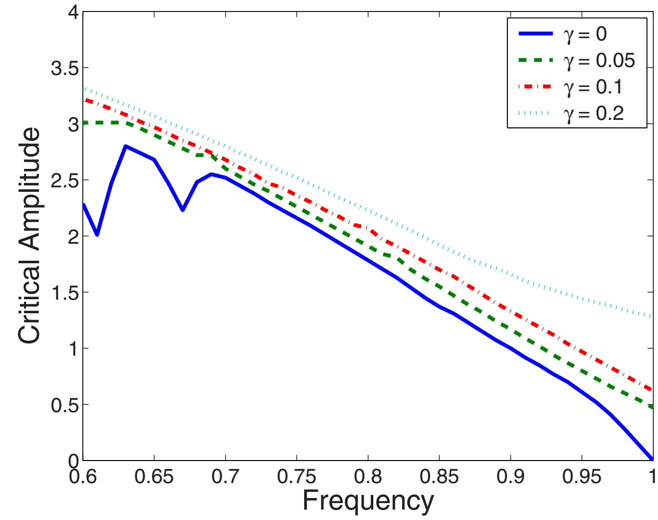

FIG. 4. (Color online) Diagrams of occurrence of critical amplitude at which supratransmission starts versus driving frequency, for the two-dimensional sine-Gordon problem (2) defined spatially in the set $[0,5]\times[0,5]$, for several values of γ. The system is harmonically perturbed on the coordinate axes.

ever, a driving amplitude of 1 manifests itself in solution amplitudes that reach the value of 6 in the farthest point of the domain D, and values of the local energy density that reach up to 30. These results obviously establish the presence of nonlinear supratransmission in the medium under study, at least for the case when the driving frequency is equal to 0.9.

At this point it is indispensable to show that the abrupt change in the behavior of solutions to the problem around a threshold value is a phenomenon that happens for every value of Ω in the forbidden band-gap region, and its occurrence does not depend on the computational parameters Δx, Δy, and Δt. Fixing all the parameters of the model, we have performed numerical experiments in order to approximate the critical amplitude at which supratransmission occurs for several fixed values of $\Delta x=\Delta y$, letting then Δt tend to zero. The results show that the associated critical amplitude converges to a fixed value A_s as Δx, Δy, and Δt tend to zero, confirming thus that the existence of the critical amplitude is independent of the computational parameters. Moreover, our experiments show that values of $\Delta x=\Delta y$ less than or equal to 0.2 and values of Δt less than or equal to $\frac{1}{10}\Delta x$ provide approximations to A_s which are correct within four decimal places.

The next step in this work is to construct a diagram of critical amplitude above which supratransmission occurs versus driving frequency for an undamped medium governed by Eq. (2), fixing the computational parameters $\Delta x=\Delta y=0.1$ and $\Delta t=0.01$, and fixing $(L,L)\in[0,L]\times[0.L]$ as the point where supratransmission is to be measured. The results are presented as the solid line in Fig. 3, and they show a resemblance with the qualitative behavior of the graph corresponding to the $(1+1)$-dimensional scenario [1], and the limiting, discrete, $(2+1)$-dimensional case investigated in Ref. [14]. This latter limiting case was obtained using a relatively large bounded, discrete system in which unboundedness was simulated through an absorbing boundary on ∂D_2, as described in Ref. [22].

Figure 3 presents diagrams of critical amplitude versus driving frequency for undamped sine-Gordon systems defined in $[0,L]\times[0,L]$, for various values of L, and relatively large frequencies. The graph shows that the critical amplitude increases as L increases, at least for most of the considered values of Ω in [0.7, 1]. We must mention here that the results obtained for $L=30$ are in excellent agreement with those of the limiting case scenario investigated in Ref. [14] through a different computational technique.

We have carried out a similar investigation in weakly damped sine-Gordon problems governed by Eq. (2), and we have likewise found the presence of the process of nonlinear supratransmission. It is not our intention to provide numerical proof of its existence here; however, we provide diagrams of critical amplitude versus driving frequency of a sine-Gordon medium defined on $[0,5]\times[0,5]$, for several values of the parameter γ. This information is given in Fig. 4, and it shows that weak damping delays the appearance of the supratransmission threshold, for values of Ω in [0.6, 1]. We must declare that we have chosen several other frequency values in [0.1, 0.6), and we have found out that, for every fixed frequency Ω, the value of the critical amplitude increases as γ increases. Moreover, our computations show that the presence of a nonzero damping coefficient results in smoother graphs of critical amplitude versus driving frequency, at least for the frequency range considered in this work.

Finally, in our investigation it is important to posses an estimate of the time it takes in order for the phenomenon of supratransmission to be observed in system (2); particularly, it is indispensable to posses an upper bound for such an instant of time, which we will denote by t_s. Figure 5 actually presents the relationship between t_s and the frequency of the driving boundary in systems governed by Eq. (2) over the spatial domain $[0,5]\times[0,5]$, for several values of the damping coefficient. Certainly, the graphs do not provide smooth

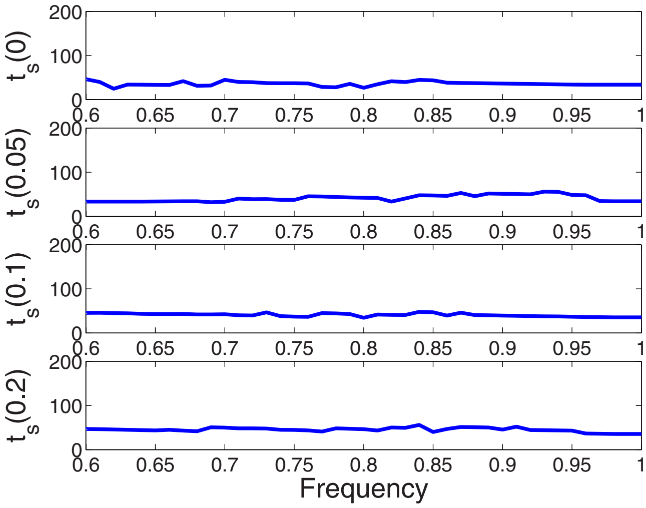

FIG. 5. (Color online) Graphs of smallest time $t_s(\gamma)$ at which supratransmission is observed in a system described by Eq. (2) versus driving frequency over the spatial domain $[0,5]\times[0,5]$, for four different values of the damping coefficient γ: 0, 0.05, 0.1, and 0.2.

relationships between the time t_s and the driving frequency. This is due to the fact that the supratransmission values employed are mere approximations; however, the importance of these results lies in the fact that t_s is clearly bounded from above, an upper bound being, for instance, $t=100$.

B. Bistability

Throughout this section, we let A_s and A_i be the nonlinear thresholds of supratransmission and infratransmission, respectively, associated with a fixed system described by Eq. (2). In other words, we let A_s be the critical amplitude above which the medium starts to absorb energy from the driving boundary, and we let A_i be the amplitude threshold below which a medium that is already absorbing energy from the boundary suddenly stops doing so. We prove here that damped sine-Gordon systems governed by Eq. (2) present these two critical amplitudes.

At this stage of our work, we will fix the driving frequency and vary the driving amplitude on an interval $[0,A_{\max}]$ which contains the supratransmission threshold. As a first step, we will measure the maximum local energy at the point (L,L) for each of the amplitudes in a regular partition of $[0,A_{\max}]$. These amplitudes will increase from zero until the supratransmission threshold is reached. After that, the driving amplitude will be decreased and the maximum local energy at (L,L) will be computed again, until we reach the infratransmission threshold. In a first computational experiment, we will fix a damping coefficient equal to 0.1, while this same parameter will be equal to 0.03 in a second trial. As a consequence of our results, we will check that the infratransmission threshold tends to zero as the damping coefficient tends to zero, a result which is in perfect agreement with the $(1+1)$-dimensional case [2].

In order to evidence the bistable behavior of the $(2+1)$-dimensional problem (2), perturbed at the boundary by a frequency Ω in the forbidden band-gap and nonnegative amplitude A_0, we drive the system at the boundary using the function

$$\phi(t) = A(t)\sin(\Omega t), \tag{12}$$

where $A(t)$ may be any of the two driving amplitude functions

$$A(t) = \begin{cases} \dfrac{A_0 t}{10}, & t \leqslant 10, \\ A_0, & t \geqslant 10, \end{cases} \tag{13}$$

and

$$A(t) = \begin{cases} \dfrac{A_s t}{10}, & t \in [0,10], \\ A_s, & t \in [10,490], \\ A_s + \dfrac{A_0 - A_s}{10}(t-490), & t \in [490,500], \\ A_0, & t \geqslant 500, \end{cases} \tag{14}$$

It is evident from the definition of function (14) that it attains the supratransmission threshold for a period of time equal to 480, after which it increases or decreases monotonically in order to reach the value A_0 in a finite time. On the other hand, Eq. (13) is always nondecreasing, and reaches its maximum value A_0 in a time period equal to 10.

Let us fix the spatial domain $[0,5]\times[0,5]$ for a two-dimensional sine-Gordon system described by Eq. (2), with damping coefficient equal to 0.1 and driving frequency 0.75. Our numerical results have shown that the supratransmission threshold for such parameters is approximately equal to 2.36; so, in a first step, we compute the maximum value of u and H at (5, 5), attained by the medium driven by Eq. (12) with amplitude function given by Eq. (13), over a time interval [0, 1000], with A_0 changing from 0 to A_s. The results are presented in Fig. 6(a), in which the arrow pointing right shows the direction of increase of A_0. Evidently, the supratransmission threshold is reached in a value close to the one obtained previously, in both the solution and the local energy density domains.

In a second stage, we choose a driving amplitude function given by Eq. (14), for several values of A_0 decreasing in the interval [0, 3], and drive system (2) for a period of time equal to 1500. The maximum values of $u(5,5)$ and $H(5,5)$ are presented also in Fig. 6(a), and it shows that a sudden decrease in the maximum amplitude of solutions and local energy density occurs around the amplitude value 1.62. We identify this new critical amplitude as the infratransmission (or lower transmission) threshold and, as in the $(1+1)$-dimensional case, we denote it by A_i.

Figure 6(b) presents the results of a similar experiment conducted on a sine-Gordon medium with damping coefficient equal to 0.03 and the same driving frequency as in the paragraph above, and it show also the presence of an infratransmission threshold. The results show that the value of the infratransmission threshold decreases as γ decreases. Figure

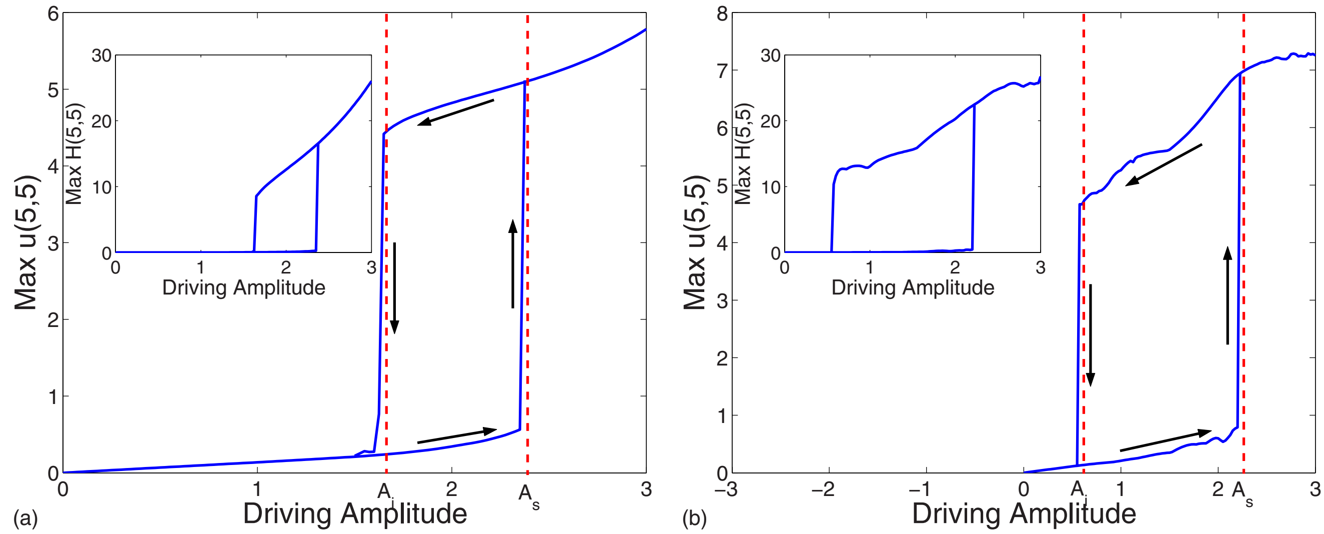

FIG. 6. (Color online) Maximum value of the solution u at the point (5, 5) to damped problem (2) defined on $[0,5]\times[0,5]$, for different driving amplitudes and a fixed driving amplitude $\Omega=0.75$. Two scenarios have been considered: $\gamma=0.1$ and (left graph) and $\gamma=0.03$ (right graph). The insets represent the corresponding graphs of maximum local energy density at the point (5, 5) versus driving amplitude.

7 in fact presents graphs of occurrence of the lower transmission amplitude versus driving frequency for several values of γ. Here, it is interesting to notice that the graph of nonlinear infratransmission is equal to zero when γ equals zero. Thus, an undamped two-dimensional sine-Gordon system which has already reached the supratransmission threshold will continue absorbing energy from the boundary as long as the driving amplitude is a positive real number. Also, it is worth noticing from Fig. 7 that the difference between the supratransmission and infratransmission functions decreases as the value of γ increases.

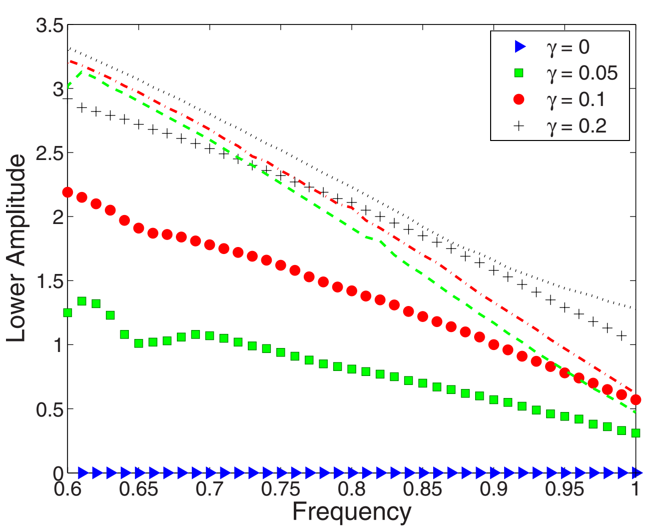

FIG. 7. (Color online) Diagrams of occurrence of the threshold value at which infratransmission occurs versus driving amplitude, for the two-dimensional sine-Gordon problem (2) defined spatially in the set $[0,5]\times[0,5]$, for several values of γ. The system is harmonically perturbed on the coordinate axes. The supratransmission thresholds for γ equal to 0.05, 0.1, and 0.2 are presented in dashed, dashed-dotted, and dotted lines, respectively.

V. APPLICATION

The purpose of this section is to show that it is possible to transmit binary information in a medium described by Eq. (2) by means of a suitable modulation of the driving boundary. For practical purposes, we focus our attention on the point (L,L) of the spatial domain, and fix the parameters $L=5$, $\gamma=0.1$, and $\Omega=0.79$, in which case the approximate values of the supratransmission and infratransmission thresholds are $A_s=2.18$ and $A_i=1.43$.

In a general framework, let us assume that the binary message $(b_1,b_2,\ldots,b_n)$ is to be transmitted into the medium of interest by a suitable modulation of the driving boundary, where each of the b_j is a digit in the set {0, 1}. We let a_0 be equal to zero, and for every $j=1,2,\ldots,n$, we define

$$a_j = b_j A_s + (1-b_j)A_i. \tag{15}$$

With this notation at hand, we let $T \gg 10$ be a real number which is a multiple of the period of the driving, and let $\tau_j = jT$ for every integer j. We define the driving amplitude function

$$A(t) = \sum_{j=1}^{n} \alpha_j(t)\chi_{[\tau_{j-1},\tau_j)}(t), \tag{16}$$

where $\chi_S(x)$ denotes the characteristic or indicator function on the set S evaluated on x, which is equal to 1 if $x\in S$, and 0 otherwise. Moreover, we let

$$\alpha_j(t) = \begin{cases} \dfrac{a_j - a_{j-1}}{10}(t-\tau_j) + a_j, & \tau_{j-1} \leqslant t < \tau_{j-1}+10, \\ a_j, & \tau_{j-1}+10 \leqslant t < \tau_j. \end{cases} \tag{17}$$

The driving function defined in Eq. (16) is a continuous function whose values oscillate in the interval $[A_i,A_s]$ for $t \geqslant T$, and it represents the transitions between the conducting

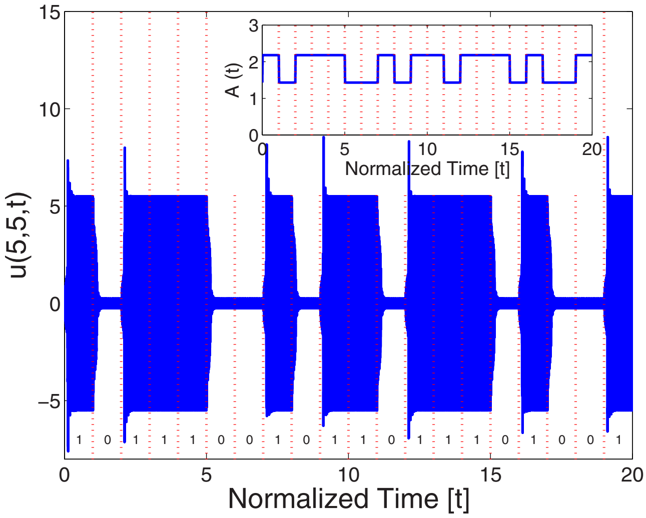

FIG. 8. (Color online) Graph of solution u of problem (2) at the point (5, 5) versus normalized time in the bounded domain $[0,5]\times[0,5]$, with a coefficient of damping equal to 0.1 and a driving frequency of 0.79, as a result of transmitting the binary message "10111001011011101001" by perturbing the driving boundary. The inset represents the graph of the time evolution of the amplitude function (16).

and insulating regimes of system (2) which are required to transmit binary bits into the medium. More concretely, for every period of time $[\tau_{j-1},\tau_j)$, the value of a_j given by Eq. (15) will be equal to A_i if $b_j=0$, or A_s if $b_j=1$. As defined by Eq. (17) and in order to avoid numerical instability, α_j will linearly change from a_{j-1} to a_j in the first ten units in the time interval $[\tau_{j-1},\tau_j)$, after which α_j will be constantly equal to a_j. In view of this, amplitude function (16) will practically take on constant values over each interval $[\tau_{j-1},\tau_j)$, those values being equal to A_i or A_s, depending on whether a bit equal to 0 or equal to 1 is to be transmitted within that interval, respectively.

In practice, we let T be equal to 250 periods of the driving boundary, and compute the time evolution of the solution u and the local energy density H at (5, 5). The results are presented in Fig. 8 for a time normalized with respect to the period T. Here, it is easy to see that the maximum amplitude of the solution at (5, 5) is approximately equal to 5.3 when a bit equal to 1 is transmitted, while a bit equal to 0 produces an amplitude smaller than 0.3. Similar qualitative remarks may be made in the graph of local energy density versus normalized time.

VI. DISCUSSION

It is worthwhile noticing that the numerical results in Ref. [2] are supported by an analytical apparatus which still does not exist in the (2+1)-dimensional scenario. However, it is important to realize that our results are qualitatively in agreement with those obtained for (1+1)-dimensional media governed by sine-Gordon equations. It is particularly interesting to point out the similarities of our results with respect to Ref. [2], especially the qualitative similarities between the graph of output amplitude versus input amplitude summarized in Fig. 6, and the numerical results reported in Fig. 8 of that work.

It was proved in Ref. [2] that a (1+1)-dimensional sine-Gordon equation defined on a closed and bounded spatial interval $[0,L]$ and subject to harmonic driving on one end, admits three qualitatively different solutions. The proof is based on the assumption that the solutions of the sine-Gordon problem studied may be expressed in the form

$$u(x,t) = 4\arctan[X(x)T(t)]. \tag{18}$$

This is a well-known technique called Lamb's substitution, which is usually employed together with the method of separation of variables in order to solve the sine-Gordon equation.

The calculations in Ref. [2] establish a well-defined correspondence between the output amplitude (that is, the amplitude measured at $x=L$) and the driving amplitude A, for values of A above certain critical value A_s which depends on the driving frequency: the nonlinear supratransmission threshold. On the other hand, for values of A less than A_s, there exist three theoretical output amplitudes derived from the three solutions obtained through Lamb's substitution. Indeed, the results in Ref. [2] present the plot of the predicted output amplitude versus A derived from the three solutions; moreover, the numerical simulations of that work establish that one of the solutions is unstable, so that only two output amplitudes coexist for values of $A<A_s$. Moreover, when damping is present, the existence of a second critical amplitude A_i is observed, below which there exists a unique output amplitude for each $A<A_i$.

On the other hand, Fig. 6 of our work presents a graph of maximum output amplitude versus driving frequency for a damped, two-dimensional sine-Gordon problem of the form (2). In this scenario, we have shown that, as in the (1+1)-dimensional case, there exist critical amplitudes A_i and A_s, with the property that two different output amplitudes coexist for driving amplitudes $A\in(A_i,A_s)$. Likewise, driving amplitudes satisfying $A<A_i$ or $A>A_s$ have associated a unique maximum output amplitude.

In view of these observations, we suspect that the (2+1)-dimensional sine-Gordon problem investigated in this article has a theory which is very similar to the (1+1)-dimensional scenario. Particularly, it is suspected that the undamped model possesses three qualitatively different solutions of which one of them is unstable. This underlying theory should be able to predict the relation between the output and the driving amplitudes presented in Fig. 6 of our work.

VII. CONCLUSIONS

In this article, we have presented numerical evidence in favor of the existence of the processes of nonlinear supratransmission and nonlinear bistability in a harmonically perturbed, two-dimensional sine-Gordon medium with a constant damping coefficient. A numerical approximation to the process of supratransmission has been provided for the undamped scenario, and predictions for several weakly undamped cases have been given in this work for high driving frequencies. Moreover, the effects of the size of a bounded domain and variations in the damping coefficient have been studied here from a computational perspective.

As a result of our study, it has been shown that the presence of damping tends to delay the appearance of both the supratransmission and infratransmission (or lower transmission) thresholds. Our results have established also that the bistability region is narrowed by the presence of damping. As a consequence, the difference between the supratransmission and infratransmission thresholds can be made arbitrarily small by taking a sufficiently large value of the damping coefficient. On the other hand, a system without damping lacks nonzero infratransmission threshold, a fact which is in perfect agreement with the theory supporting the $(1+1)$-dimensional scenario [2].

Our numerical results have been produced through a computational method to approximate solutions of a generic class of $(2+1)$-dimensional Klein-Gordon equations, which has an energy scheme associated with it that consistently approximates the rate of change of the energy of the system. Most of the conclusions drawn in this work have been verified in both the domain of solutions and the domain of the local energy density, obtaining results which are in perfect agreement.

As an application of our observations, we have proved that a suitable manipulation of the driving amplitude in a sine-Gordon system may result in a perfect transmission of binary information. This fact is established by considering a damped sine-Gordon system subject to a harmonic perturbation with a fixed frequency in the forbidden band-gap, and varying the driving amplitude conveniently between the supratransmission and infratransmission thresholds. Results for both the solution of the system and its local energy density yield consistent conclusions.

ACKNOWLEDGMENTS

The author wishes to thank the anonymous reviewers for their invaluable comments which invariably led to a substantial improvement of this work. Also, he wishes to acknowledge support from Dr. Álvarez Rodríguez, dean of the Faculty of Sciences of the Universidad Autónoma de Aguascalientes, and from Dr. Avelar González, head of the Office for Research and Graduate Studies of the same university. The present work represents a set of partial results under Project No. PIM08-1 at this institution.

[1] F. Geniet and J. Leon, Phys. Rev. Lett. **89**, 134102 (2002).
[2] R. Khomeriki and J. Leon, Phys. Rev. E **71**, 056620 (2005).
[3] D. Chevriaux, R. Khomeriki, and J. Leon, Phys. Rev. B **73**, 214516 (2006).
[4] R. Khomeriki, S. Lepri, and S. Ruffo, Phys. Rev. E **70**, 066626 (2004).
[5] S. Zaitsev, R. Almog, O. Shtempluck, and E. Buks, in Proceedings of the 2005 International Conference on MEMS, NANO, and Smart Systems (IEEE, Banff, Alberta, Canada, 2005), pp. 387–391.
[6] D. Chevriaux, R. Khomeriki, and J. Leon, Mod. Phys. Lett. B **20**, 515 (2006).
[7] L. Wei, S. Song, and Y.-N. Wang, Opt. Laser Technol. **37**, 432 (2005).
[8] H. G. Winful, J. H. Marburguer, and E. Garmire, Appl. Phys. Lett. **35**, 379 (1979).
[9] H. S. J. van der Zant, M. Barahona, A. E. Duwel, E. Trías, T. P. Orlando, S. Watanabe, and S. H. Strogatz, Physica D **119**, 219 (1998).
[10] N. K. Martinov and N. K. Vitanov, J. Phys. A **25**, L419 (1992).
[11] N. K. Martinov and N. K. Vitanov, J. Phys. A **25**, 3609 (1992).
[12] N. K. Martinov and N. K. Vitanov, J. Phys. A **27**, 4611 (1994).
[13] N. K. Vitanov, Proc. R. Soc. London, Ser. A **454**, 2409 (1998).
[14] J. E. Macías-Díaz, Phys. Rev. E **77**, 016602 (2008).
[15] K. Djidjeli, W. G. Price, and E. H. Twizell, J. Eng. Math. **29**, 347 (2004).
[16] Q. Sheng, A. Q. M. Khaliq, and D. A. Voss, Math. Comput. Simul. **68**, 355 (2005).
[17] S. Flach, K. Kladko, and C. R. Willis, Phys. Rev. E **50**, 2293 (1994).
[18] V. L. Pokrovsky and A. L. Talapov, Phys. Rev. Lett. **42**, 65 (1979).
[19] B. Horovitz, Phys. Rev. Lett. **46**, 742 (1981).
[20] A. Sánchez, A. R. Bishop, and E. Moro, Phys. Rev. E **62**, 3219 (2000).
[21] J.-G. Caputo, N. Flytzanis, Y. Gaididei, and E. Vavalis, Phys. Rev. E **54**, 2092 (1996).
[22] F. Geniet and J. Leon, J. Phys.: Condens. Matter **15**, 2933 (2003).